Scientia Horticulturae 339 (2025) 113901

Contents lists available at ScienceDirect

Scientia Horticulturae

journal homepage: www.elsevier.com/locate/scihorti

Research Paper

Genetic mapping reveals a major locus for red leaf blotch tolerance in almond

Alejandro Calle [a,*], Gemma Pons-Solé [b], Núria Real [b], Jordi Luque [b], Iban Eduardo [c,d], Laura Torguet [a], Ignasi Batlle [e], Xavier Miarnau [a]

[a] IRTA, Fruit Production, Fruitcentre, 25003 Lleida, Catalonia, Spain
[b] IRTA, Sustainable Plant Protection, Centre de Cabrils, 08348 Cabrils, Catalonia, Spain
[c] IRTA, Centre de Recerca en Agrigenòmica (CRAG), CSIC-IRTA-UAB-UB, Cerdanyola del Vallès (Bellaterra), Barcelona 08193, Spain
[d] Centre for Research in Agricultural Genomics (CRAG) CSIC-IRTA-UAB-UB, Campus UAB, Edifici CRAG, Cerdanyola del Vallès (Bellaterra), Barcelona 08193, Spain
[e] IRTA, Fruit Production, Mas Bové, 43120 Constantí, Catalonia, Spain

ARTICLE INFO

Keywords:
Crop disease
Polystigma amygdalinum
Prunus amygdalus
Resistance genes
Tolerance

ABSTRACT

Red leaf blotch (RLB) of almond, caused by the fungus *Polystigma amygdalinum*, is a common foliar disease in Mediterranean and Middle East countries. RLB symptoms are characterized by orange spots on leaves that eventually lead to early defoliation, reducing tree photosynthetic activity and fruit production. This study aimed to investigate the genetic basis of RLB tolerance in almond. For this purpose, an F_1 population (N=79) derived from a cross between two cultivars with different levels of disease tolerance ('Tarraco', highly susceptible; and 'Vairo', tolerant) was phenotyped for disease severity and incidence over four years and genotyped with the almond Axiom™ 60K SNP array. Linkage maps were constructed and used for QTL analyses. A major QTL (*qP-RLB-3.1*^{m}), detected across all years and accounting for up to 21 and 31% of phenotypic variation for disease incidence and severity respectively, was found at the lower end of linkage group (LG) 3. Minor QTLs, only detected in particular years and explaining low percentages of the phenotypic variations, were also detected on LGs 1, 7, and 8. *qP-RLB-3.1*^{m} was targeted for haplotype analysis in the individuals of the population, and in 19 almond cultivars with different levels of disease susceptibility, revealing an interesting allele associated with increased disease tolerance. In the region spanning *qP-RLB-3.1*^{m}, there were 505 annotated genes in the almond reference genome. Fourty-nine of them were related to plant defense mechanisms in other species. The possible involvement of these genes and the implementation of marker-assisted selection strategies in almond breeding programs are discussed.

1. Introduction

Red leaf blotch (RLB) of almond (*Prunus amygdalus* Batsch), caused by the ascomycete fungus *Polystigma amygdalinum* P. F. Cannon, stands as one of the most widespread foliar diseases affecting almond crops in the Mediterranean basin and Middle Eastern regions, where its prevalence is notable (Cannon, 1996; Ollero-Lara et al., 2019). Particularly in Spain, RLB has notably spread in recent years along the Mediterranean coast (East) and the Ebro Valley (Northeast) areas (Miarnau et al., 2021). This increasing incidence has been linked to i) the introduction of the crop into new climatic regions suitable for RLB development, ii) the establishment of new intensive plantations under irrigation conditions; and iii) the use of cultivars more susceptible to the disease. It is thought that the combination of the above factors may have created favorable conditions for the spread of RLB (Ollero-Lara et al., 2019; Miarnau et al., 2021).

RLB is specific to almond leaves (Banihashemi 1990), which is shown as spots of different shapes and sizes (circular to elliptical, mostly up to 25 mm in diameter) on both leaf surfaces. These lesions, consisting of pathogen stromata interspersed within the host tissue, appear after an incubation period that can be extended up to 10 weeks (Saad and Masannat, 1997; Zúñiga et al., 2020). The blotches initially appear in spring as yellowish spots, turning into orange-reddish, and lately darkening into blackish-brown spots. In the stromata, spermatia form during summer, and perithecia later develop during autumn and winter, after leaf fall (Cannon, 1996; Habibi & Banihashemi, 2016). Under favorable

* Corresponding author.
E-mail address: alejandro.calle@irta.cat (A. Calle).

https://doi.org/10.1016/j.scienta.2024.113901
Received 17 July 2024; Received in revised form 6 November 2024; Accepted 10 December 2024
Available online 17 December 2024
0304-4238/© 2024 The Authors. Published by Elsevier B.V. This is an open access article under the CC BY license (http://creativecommons.org/licenses/by/4.0/).

environmental conditions in spring, particularly with mild temperatures and the hydration of fallen leaves, ascospores are released, leading to infections on new almond leaves (Pons-Solé et al., 2023; 2024). In heavily affected orchards, early defoliation of trees may occur, thus leading to a subsequent decline in tree photosynthesis and yield (Habibi & Banihashemi, 2016; López-López et al., 2016).

RLB control has usually relied on three distinct strategies: (i) orchard management practices, aimed at reducing inoculum levels by removing infected fallen leaves or facilitating their decomposition through urea applications (Cannon 1996; López-Moral et al., 2022); (ii) the use of more tolerant cultivars (Miarnau et al., 2021); and (iii) fungicide applications to prevent RLB infections on new leaves (Torguet et al., 2022). While fungicide applications are the most commonly used strategy, reducing their applications is desirable for its environmental implications, as has been recently promoted by the European Commission through the European Green Deal (European Commission, 2019). Therefore, breeding cultivars with a higher tolerance level to RLB in almond has been targeted as a long-term strategy for disease control.

Variations in susceptibility to RLB within the almond germplasm have been previously reported (Egea et al., 1984; Ollero-Lara et al., 2019; Miarnau et al., 2021). For instance, 'Mardía' and 'Vairo' cultivars have shown lower susceptibility compared to others like 'Tuono' and 'Tarraco' (Miarnau et al., 2021). However, due to the limited distribution of RLB, its host specificity, and the inability to grow in artificial media, the understanding of disease tolerance levels in almond germplasm remains limited (Cannon 1996). Additionally, little research has been conducted regarding the genetic and biochemical mechanisms underlying plant-pathogen interactions involving RLB. Zúñiga et al. (2019) suggested a significant role of the phenylpropanoid pathways in the defense response against RLB by showing that early production of lignin may serve as a primary mechanism for controlling the spread of *P. amygdalinum* within almond leaf tissues. Thus, the characterization of genome regions or genes associated with disease tolerance has become a primary focus in improving almond breeding (Batlle et al., 2017). These resources could assist in the near future as the foundation for the development and implementation of marker-assisted selection (Aranzana et al., 2019), by enabling seedling selection in the early stages of plant development.

Given the limited research on RLB and its widespread occurrence, this study aimed at exploring the genetic basis of *P. amygdalinum* tolerance in almonds. To achieve this, an F_1 population arising from the cross between two parentals, displaying variation in disease tolerance, was genotyped and phenotyped for disease susceptibility over four years. Quantitative trait locus (QTL) analyses were performed, and the haplotypes in the most important genomic region identified were studied in a collection of almond cultivars. Finally, a candidate gene analysis was also performed in this major region using the almond reference genome 'Texas' v3.0-F1 (Castanera et al., 2024).

2. Materials and methods

2.1. Plant material

An F_1 population derived from the cross between 'Tarraco' and 'Vairo' (T×V; N=79) was used in this study. Both parents are breeding cultivars released by IRTA (Vargas et al., 2008), showing different levels of susceptibility to RLB. 'Tarraco' exhibits a high susceptibility level, whereas 'Vairo' shows very low susceptibility (Miarnau et al., 2021). All seedlings and parentals were grafted onto 'Garnem®' rootstocks and planted as central axis at 4 × 1.5 m spacing in 2016. The population was maintained at the IRTA Les Borges Blanques Experimental Station (Lleida, Spain; 41°30'31"N, 0°51'10"E) under standard agricultural practices in the area regarding irrigation, pruning, soil management, and fertilization. No fungicide treatments were applied during the experimental period to allow natural RLB infections.

2.2. Disease phenotyping and data analysis

Evaluations of RLB symptoms were conducted annually from July to August over four years (2018, 2019, 2020, and 2022). During the first two years, for each tree in the population, disease incidence and severity were evaluated by collecting 25 fully expanded leaves, from the outer canopy, encompassing various heights and orientations. In 2020 and 2022, evaluations were conducted on 50 leaves per tree. Disease incidence was quantified as the percentage of leaves exhibiting at least one identifiable RLB lesion, regardless of size. To evaluate disease severity, collected leaves were visually categorized into five groups according to Miarnau et al. (2021): Group 0 (0% of leaf surface affected), Group 1 (1–10%), Group 2 (11–20%), Group 3 (21–50%), and Group 4 (>50%). A mean leaf severity index for each genotype was calculated using the weighted average of the midpoint percentage for each class. For the parental cultivars ('Tarraco' and 'Vairo'), disease incidence and severity were evaluated as in the population but using four trees per genotype. In addition, the broad-sense heritability (H^2) for disease incidence and severity was calculated using the following formula: $H^2 = \frac{\sigma_g^2}{\sigma_g^2 + \frac{\sigma_e^2}{n}}$; where σ_g^2 is the variance of the genotype effect, σ_e^2 is the variance of the residual term, and n represents the number of years.

Statistical analyses were conducted to determine the correlations between disease indices and years. Spearman's correlation coefficients were calculated for the relationships between traits across years. Additionally, the Shapiro–Wilk's W statistic ($p < 0.05$) was used to assess the normal distribution of each trait in each annual dataset. All statistical analyses were calculated using R software 4.3.1 (R Core Team, 2021) and specifically the packages '*lme4*' (Bates et al., 2015) and '*psych*' (Revelle, 2024).

2.3. Genotyping and linkage mapping

Individuals and parentals from the T×V population were genotyped using the almond Axiom™ 60K SNP array (Duval et al., 2023). Total genomic DNA was extracted for each genotype from young leaves following the CTAB protocol in 96-well plates (Doyle & Doyle, 1990). Genotyping was conducted using the Axiom GeneTitan system (ThermoFisher Scientific; Waltham, USA) at the INRAE Gentyane platform (Clermont-Ferrand, France). The SNP genotypes were then analyzed and filtered using the Axiom Analysis Suite software following the best practices workflow settings (ThermoFisher, 2017).

Linkage map construction was performed using JoinMap® 5 software (van Ooijen, 2018) using the pseudo-testcross strategy (Grattapaglia & Sederoff, 1994). Three genetic maps were constructed, including one for each parental ('Tarraco' and 'Vairo') and the integrated map (T×V). For map construction, the minimum independence of logarithm of odd (LOD), the maximum likelihood mapping algorithm, and the Kosambi mapping function (Kosambi, 1944) were used. For the parental maps, only markers that were heterozygous in one parent and homozygous in the other were used. For the T×V map, all segregating markers in both parentals were used. Given the high number of markers mapped in the same genetic position, a single SNP was used to represent each group of co-segregating markers or bin.

2.4. QTL and haplotype analyses

QTL mapping was conducted for disease incidence and severity using the three genetic maps available ('Tarraco', 'Vairo', and 'T×V'). Data from each year were analyzed independently, as well as the average value over the four years. MapQTL® 6 software (van Ooijen, 2009) was used for both interval mapping (Lander & Botstein, 1989) and multiple QTL mapping (MQM) methods (Jansen, 1994). To determine the LOD significance threshold for each QTL within every linkage group (LG), a permutation test was conducted at a significance level of 95%

($p < 0.05$), employing 10.000 permutations (Lander & Botstein 1989; van Ooijen 1992). Given the similarity in the LOD significance threshold for each QTL, a LOD threshold equal or higher than 3 was used for all analyses. Therefore, a QTL interval was considered as a region with a LOD $\geq$ 3. Graphical representations of LGs and QTLs were generated using MapChart software (Voorrips 2002). We defined a QTL as consistent if it was detected each year. QTLs were named based on the recommendations for standard QTL nomenclature as reported in the Genome Database for Rosaceae (e.g: *qP-RLB4.3*^{m}: where q = quantitative trait; P = *Prunus*; RLB = red leaf blotch; 4 = chromosome number; 3 = 3rd chronological QTL for this trait reported in this chromosome; and m = same QTL identified in multiple years) (Jung et al., 2019). The physical positions of QTLs are based on the 'Texas' almond genome v3.0-F1 (Castanera et al., 2024).

Two SNPs from the genomic region of *qP-RLB-3.1*^{m} were selected for the haplotype analysis (AX-586074286 and AX-586076177). For each haplotype combination, mean phenotyped values for those individuals carrying the same genotypes were estimated for disease incidence and severity. Statistical analyses were performed by using ANOVA to estimate the mean comparisons among phenotypic values of each segregating class within each population using R (R Core Team, 2021). Additionally, the genotypes for these two selected SNPs were also investigated in 19 cultivars in which different susceptibility levels to disease were previously reported (Miarnau et al., 2021). Cultivar genotypes were obtained from the almond Axiom™ 60K SNP array (Pérez de los Cobos et al., 2023).

2.5. Candidate gene analyses

To study the positional candidate genes, we obtained the annotation information from the 'Texas' reference genome v3.0-F1 (Castanera et al., 2024), in the genomic region of *qP-RLB-3.1*^{m}. This region (Chr03: 25.59 to 29.10 Mbp) was defined based on the overlapping QTLs detected across multiple years in both parental and T×V maps. For each gene, a comprehensive search of scientific literature and genetic databases was conducted to uncover information related to their potential involvement in plant defense mechanisms.

3. Results

3.1. Disease incidence and severity

Disease incidence and severity were assessed in the parental cultivars ('Tarraco' and 'Vairo') and the individuals from the T×V population (Fig. 1; Supplementary Table 1). The results indicated that 'Tarraco' exhibited greater disease incidence than 'Vairo' (83.4% and 72.5% in average, respectively). Similarly, 'Tarraco' displayed higher disease severity (29.2% and 9.7% in average, respectively). This trend was consistent across all evaluated years except for 2022, when 'Vairo' displayed a slightly higher disease occurrence than 'Tarraco' (77.0% and 73.5%, respectively) (Supplementary Table 1).

Within the T×V population, mean disease incidence over the four years ranged from 52.0 to 93.5%, and disease severity from 6.1 to 35.7% (Fig. 1). Disease data remained consistent across the years, particularly in 2018, 2019, and 2022. During these three years, the average population incidence ranged from 73.3% to 78.1%, and severity ranged between 8.1% and 18.0%. However, in 2020, a notable increase in disease incidence was observed, with the most tolerant individual of the T×V population showing an incidence of 68%, and the population's mean reaching 97.2%. Disease severity behaved similarly, with a mean value of 32.8% for that year (Fig. 1).

The distribution of traits revealed that only disease incidence in 2018 (W=0.969; p=0.060) and 2022 (W=0.970; p=0.068) followed a normal distribution. For disease incidence in 2019 and 2020, as well as disease severity across all assessed years, deviations from normality were observed. The correlation between years for incidence and severity indexes ranged between 0.84 and 0.90. However, in 2020, there was a notable deviation, with a correlation between these two indices of 0.38 (Supplementary Fig. 1). There was an absence of correlation between both phenotyped variables across different years. Nevertheless, the broad-sense heritability (H^2) was moderately high for both traits, with values of 0.55 for incidence and 0.61 for severity.

3.2. Genotyping and linkage mapping

From the 60.581 SNPs of the almond Axiom™ 60K SNP array, a total of 2.286 were selected for linkage mapping. Of them, 1.035 were heterozygous in 'Tarraco', 619 in 'Vairo', and the remaining 632 were found to be heterozygous in both parentals. After map construction, the parental linkage maps for 'Tarraco' and 'Vairo' comprised 244 and 251 markers, distributed in eight LGs and spanning total genetic lengths of 372.3 and 444.1 cM, respectively (Supplementary Tables 2 and 3). The average distance between markers was 1.59 and 1.91 cM for 'Tarraco' and 'Vairo', respectively. In both parentals, the largest number of markers were mapped on LG1, which was also the largest linkage group. In the T×V map, a total of 541 SNPs were mapped, spanning a genetic distance of 448.8 cM, with an average distance between markers of 0.85 cM (Supplementary Tables 2 and 3). All developed maps exhibited whole genome coverage, with average physical distance between markers of 773 Kbps for 'Tarraco', 729 Kbps for 'Vairo', and 423 Kbps

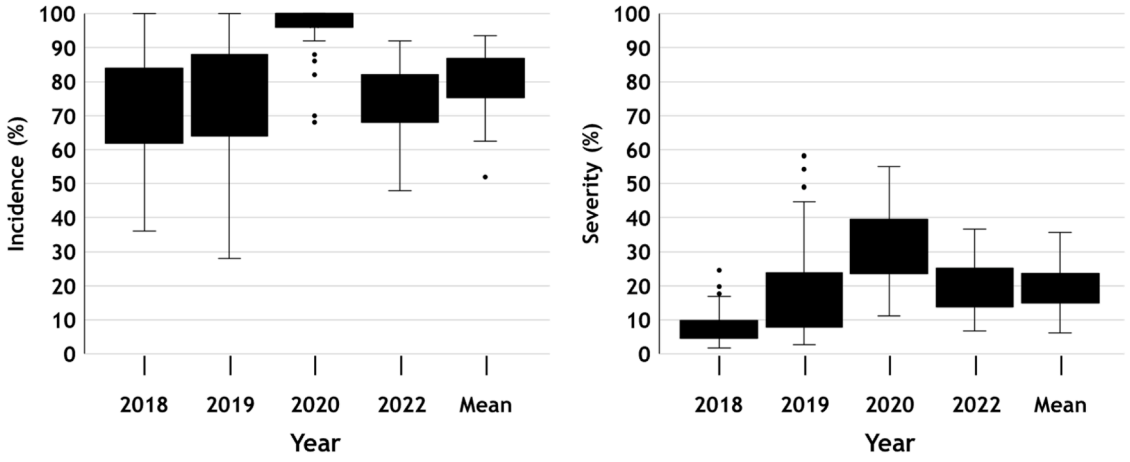

Fig. 1. Disease incidence and severity in the 'Tarraco' × 'Vairo' population for each phenotyped year and the average value over the four years. The top and bottom sides of the box indicate the 25th and 75th percentile, respectively. Whiskers represent the lower and upper extreme values. Outlier samples are indicated by dots.

for T×V.

3.3. QTL mapping

Considering all the phenotyped years, both disease indexes, and the three analyzed maps, a total of 38 QTLs linked with disease incidence and severity were identified (18 related to incidence and 20 to severity; Table 1). Among these, 14 were mapped in the 'Tarraco' map, 10 in the 'Vairo' map, and 14 in the T×V map (Fig. 2). Despite the large number of detected QTLs, only one consistent QTL (*qP-RLB-3.1*^{m}), representing 18 individual QTLs, was detected on the lower part of LG3 (Fig. 2). This region spanned from 28.2 to 43.7 cM in the 'Tarraco' map, 38.8 to 54.3 cM in the 'Vairo' map, and 37.0 to 49.7 cM in the T×V map, corresponding to the interval between 21.86 to 30.26 Mbps on chromosome 3 (total physical interval covered by all QTLs identified in this region). This QTL was detected across all years and showed percentages of phenotypic variation for disease incidence ranging from 18.2 to 21.5% and LOD scores between 3.6 and 5.2. Similarly, for disease severity, the phenotypic variation of *qP-RLB-3.1*^{m} varied from 19.2 to 31.1% with LOD scores ranging from 4.6 to 7.4 (Table 1).

In addition to *qP-RLB-3.1*^{m}, QTLs mapped on particular years and on specific maps were also detected (Table 1; Fig. 2). This is the case of *qP-RLB-1.1* detected on 'Tarraco', 'Vairo', and T×V maps within the same physical interval (Chr01: 10.03–11.75 Mbps). This QTL, detected for both disease incidence and severity, was observed in 2020 and mean data of the four years with LOD scores ranging from 3.5 to 5.1 and percentages of variance explained (PVE) between 17.8 to 21.4%. Another QTL on LG1 (*qP-RLB1.2*) was detected for disease incidence on 'Tarraco' (35.9–37.2 cM) and T×V (43.7–51.4 cM) maps in 2018, with LOD scores close to the threshold (3.0) and PVE not exceeding 17% (Table 1). Similarly, another QTL (*qP-RLB-7.1*) mapped on both parental maps and the T×V, spanning from 19.19 to 22.45 Mbps of chromosome 7, was detected for disease severity in 2020 with LOD scores ranging from 3.5 to 3.6 and PVE from 17.9 to 18.8% (Table 1; Fig. 2). Moreover, on LG8, two QTLs (*qP-RLB-8.1* and *qP-RLB8.2*) were also identified (Table 1; Fig. 2). *qP-RLB-8.1* was exclusively detected during the 2022 year for disease incidence and severity in the 'Tarraco' and T×V maps, with PVE between 17.0 to 17.4% and LOD scores not surpassing 3.3, whereas *qP-RLB8.2* was also detected uniquely in the 'Tarraco' and T×V maps but in this case only for disease incidence (PVE=16.9-17.6; LOD=3.1-3.3) (Table 1).

3.4. Haplotype analyses

To investigate how specific allele combinations within the major QTL *qP-RLB3.1*^{m} could influence disease susceptibility and incidence, a haplotype analysis was conducted. Two markers spanning this region (AX-586074286 and AX-586076177), and heterozygous in both parentals, were selected for haplotype construction.

In the individuals of the T×V population, three segregation classes were observed based on the genotypes of these markers (AA|AA, AB|AB, and BB|BB; AX-586074286|AX-586076177 genotypes, respectively) (Fig. 3). Individuals with AA genotype for both markers exhibited the lowest average of disease incidence (75.5 ± 7.8%) and severity (15.5 ±

Table 1
Summary of all detected QTLs for disease incidence and severity in 'Tarraco', 'Vairo', and 'Tarraco' × 'Vairo' maps.

Trait	Year	Map	QTL name	LG	Genetic position	Physical position (Mbp)[1]	Cofactor SNP	Max LOD	Average LOD	PVE[2]
Incidence	2018	Tarraco	qP-RLB-1.2	1	35.9-37.2	Chr1: 31.77 - 32.78	AX-586028361	3.1	3.1	17.0
	2018	T×V	qP-RLB-1.2	1	43.7-54.1	Chr1: 31.77 - 36.47	AX-586028155	3.1	3.0	16.6
	2019	Tarraco	qP-RLB-3.1^{m}	3	34.3-43.7	Chr3: 24.84 - 30.18	AX-586076641	4.2	3.7	20.1
	2019	T×V	qP-RLB-3.1^{m}	3	38.5-49.7	Chr3: 24.05 - 30.18	AX-586076641	3.9	3.4	18.5
	2019	Vairo	qP-RLB-3.1^{m}	3	42.4-49.1	Chr3: 23.97 - 29.19	AX-586074923	3.6	3.5	18.8
	2022	Tarraco	qP-RLB-3.1^{m}	3	28.2-43.7	Chr3: 21.86 - 30.18	AX-586076641	5.2	3.9	20.7
	2022	Tarraco	qP-RLB-8.1	8	25.3-26.6	Chr8: 21.55 - 21.66	AX-586148369	3.3	3.2	17.4
	2022	T×V	qP-RLB-3.1^{m}	3	38.5-49.7	Chr3: 24.05 - 30.18	AX-586076641	5.0	3.9	21.5
	2022	T×V	qP-RLB-8.1	8	35.1-37.3	Chr8: 21.55 - 22.36	AX-586148369	3.3	3.2	17.2
	2022	Vairo	qP-RLB-3.1^{m}	3	38.8-54.3	Chr3: 23.12 - 30.26	AX-586076005	4.3	4.0	21.4
	Mean	Tarraco	qP-RLB-1.1	1	11.2-17.7	Chr1: 9.53 - 12.19	AX-586019700	3.5	3.3	17.8
	Mean	Tarraco	qP-RLB-3.1^{m}	3	34.3-43.4	Chr3: 24.84 - 30.18	AX-586076641	4.3	3.5	18.9
	Mean	Tarraco	qP-RLB-8.2	8	48.8-50.1	Chr8: 27.21 - 27.32	AX-586154585	3.3	3.2	17.6
	Mean	T×V	qP-RLB-1.1	1	11.6-17.3	Chr1: 9.53 - 11.75	AX-586018561	3.8	3.5	18.9
	Mean	T×V	qP-RLB-3.1^{m}	3	39.0-47.1	Chr3: 24.05 - 29.75	AX-586076641	4.0	3.6	19.4
	Mean	T×V	qP-RLB-8.2	8	51.2-56.0	Chr8: 26.23 - 27.32	AX-586154585	3.1	3.1	16.9
	Mean	Vairo	qP-RLB-1.1	1	12.6-19.3	Chr1: 9.69 - 11.75	AX-586018561	3.8	3.6	19.5
	Mean	Vairo	qP-RLB-3.1^{m}	3	42.4-54.3	Chr3: 23.97 - 30.26	AX-586074923	3.6	3.4	18.2
Severity	2019	Tarraco	qP-RLB-3.1^{m}	3	29.5-43.7	Chr3: 23.44 - 30.18	AX-586076641	6.1	5.4	27.6
	2019	T×V	qP-RLB-3.1^{m}	3	37.0-49.7	Chr3: 23.97 - 30.18	AX-586073165	6.1	5.2	26.9
	2019	Vairo	qP-RLB-3.1^{m}	3	38.8-54.3	Chr3: 23.12 - 30.26	AX-586074923	6.0	5.1	26.4
	2020	Tarraco	qP-RLB-1.1	1	8.7-17.7	Chr1: 7.70 - 12.19	AX-586018554	3.6	3.3	18.1
	2020	Tarraco	qP-RLB-3.1^{m}	3	28.2-43.7	Chr3: 21.86 - 30.18	AX-586075383	4.0	3.6	19.2
	2020	Tarraco	qP-RLB-7.1	7	26.0-39.2	Chr7: 19.19 - 22.45	AX-586135679	3.6	3.3	17.9
	2020	T×V	qP-RLB-1.1	1	8.0-33.4	Chr1: 7.63 - 25.45	AX-586018980	4.7	3.6	19.2
	2020	T×V	qP-RLB-3.1^{m}	3	39.1-49.7	Chr3: 24.05 - 30.18	AX-586075383	4.6	4.1	21.8
	2020	T×V	qP-RLB-7.1	7	30.3-36.2	Chr7: 19.96 - 20.70	AX-586135679	3.6	3.5	18.8
	2020	Vairo	qP-RLB-1.1	1	13.9-39.9	Chr1: 10.03 - 25.48	AX-586018978	4.6	3.8	20.5
	2020	Vairo	qP-RLB-3.1^{m}	3	43.4-54.3	Chr3: 25.40 - 30.26	AX-586076903	4.7	4.4	23.0
	2020	Vairo	qP-RLB-7.1	7	33.8-41.6	Chr7: 19.73 - 20.70	AX-586135621	3.5	3.4	18.4
	2022	Tarraco	qP-RLB-8.1	8	25.3-25.6	Chr8: 21.55 - 21.66	AX-586148369	3.2	3.1	17.0
	2022	T×V	qP-RLB-8.1	8	30.9-36.3	Chr8: 20.10 - 21.14	AX-586148369	3.2	3.1	17.0
	Mean	Tarraco	qP-RLB-1.1	1	8.7-18.6	Chr1: 7.70 - 12.25	AX-586018554	4.1	3.6	19.4
	Mean	Tarraco	qP-RLB-3.1^{m}	3	28.2-43.7	Chr3: 21.86 - 30.18	AX-586075383	7.1	6.2	31.1
	Mean	T×V	qP-RLB-1.1	1	8.3-18.9	Chr1: 7.67 - 12.10	AX-586018578	5.1	4.0	21.0
	Mean	T×V	qP-RLB-3.1^{m}	3	37.0-49.7	Chr3: 23.97 - 30.18	AX-586074923	7.2	5.8	29.0
	Mean	Vairo	qP-RLB-1.1	1	4.8-20.6	Chr1: 5.73 - 12.10	AX-586018578	5.1	4.1	21.4
	Mean	Vairo	qP-RLB-3.1^{m}	3	38.8-54.3	Chr3: 23.12 - 30.26	AX-586074923	7.4	6.2	30.7

[1] Physical position based on the 'Texas' v3.0-F1 almond genome (Castanera et al., 2024).
[2] PVE: Percentage of variances explained.

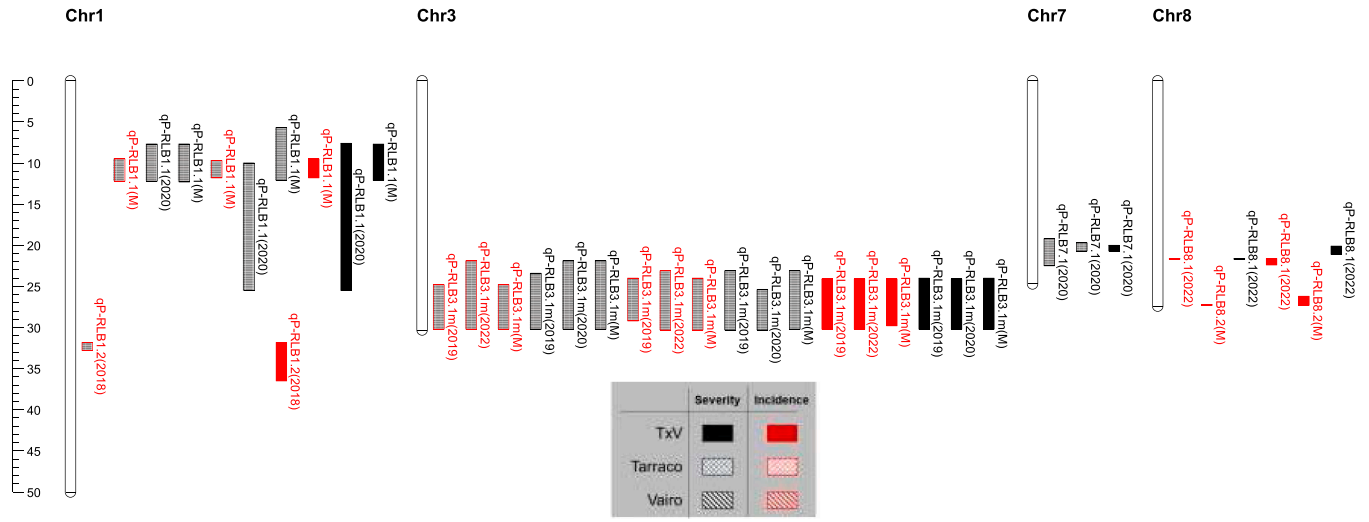

Fig. 2. Physical position (Mbp) of detected QTLs in the 'Texas' v3.0-F1 almond genome. QTL name and detected year (2018, 2019, 2020, 2022, M: Multiyear) is included.

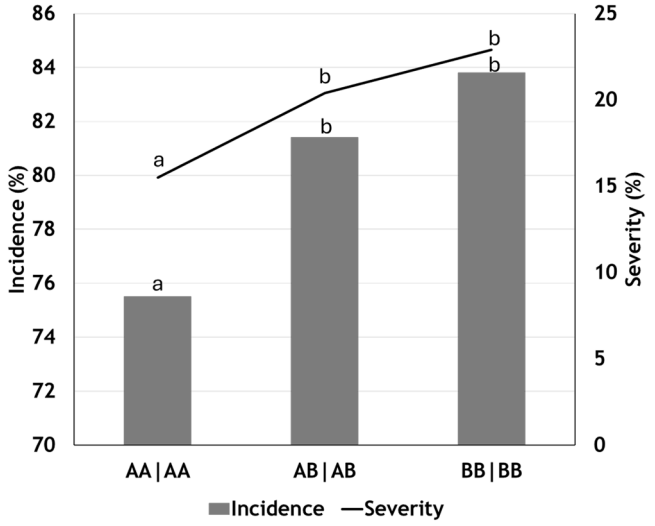

Fig. 3. Mean phenotypic values of disease incidence and severity in the three segregating classes observed among the 'Tarraco' × 'Vairo' individuals for the two SNP markers used for haplotype construction (AX-586074286 and AX-586076177). Significant differences between classes are marked by different letters ($p < 0.05$).

4.7%). Conversely, those individuals with the BB genotype in both markers showed the highest mean values for disease incidence (83.8 ± 7.7%) and severity (22.9 ± 5.9%). Meanwhile, individuals with AB genotypes for both markers (as parentals) had slightly lower disease incidence and severity compared to those with BB genotypes (Incidence = 81.4 ± 7.6%; severity = 20.4 ± 6.4%) (Fig. 3). Statistical differences between the mean phenotype values of AA|AA and the two remaining classes (AB|AB and BB|BB) were reported.

The relationships between haplotypes and susceptibility levels were also studied in 19 almond cultivars with known susceptibility to RLB (Table 2). Among these, only 'Mardía', exhibiting the highest level of disease resistance, was found to carry out AA genotypes for both markers. However, in other cultivars spanning from low tolerance to high susceptibility levels, no consistent patterns linking genotypes with susceptibility were observed.

Table 2
Genotypes for AX-586074286 and AX-586076177 markers in 19 almond cultivars showing different levels of susceptibility to *Polystigma amygdalinum*.

Genotype	AX-586074286	AX-586076177	Susceptibility
'Mardía'	AA	AA	Highly tolerant
'Marta'	BB	AA	Tolerant
'Ferraduel'	BB	AA	Tolerant
'Ferragnes'	AB	AB	Tolerant
'Constanti'	BB	AA	Tolerant
'Belona'	BB	AB	Tolerant
'Lauranne'	AB	AB	Tolerant
'Vairo'	AB	AB	Tolerant
'Penta'	AB	AB	Moderately susceptible
'Tardona'	AA	AB	Moderately susceptible
'Masbovera'	AB	AB	Moderately susceptible
'Glorieta'	AB	AA	Moderately susceptible
'Francoli'	BB	AA	Moderately susceptible
'Marcona'	BB	AB	Moderately susceptible
'Soleta'	BB	AA	Susceptible
'Marinada'	AA	AB	Susceptible
'Desmayo Largueta'	AB	AA	Susceptible
'Guara'	BB	AA	Highly susceptible
'Tarraco'	AB	AB	Highly susceptible

3.5. Candidate gene analysis

Functional analysis was performed on the genomic region of the 'Texas' genome v3.0-F1, which encompasses the major QTL identified in this study (*qP-RLB3.1*^{m}; Chr03: 25.59 to 29.10 Mbps), aiming to find potential candidate genes associated with RLB resistance in almond. A total of 505 genes were predicted within this region (Supplementary Table 4). Among them, 136 (27%) resulted in uncharacterized proteins, while for the remaining predicted genes (N=369; 73%), annotations indicated involvement in different pathways. In-depth analysis of these genes revealed the presence of 49 genes with annotations related to plant defense mechanisms (Table 3). Among these, annotations such as receptor-like protein kinase or cinnamoyl-CoA reductase-like were identified.

4. Discussion

The large number of seedlings generated annually in almond breeding programs underscores the importance of investigating the main kernel quality and agronomical traits, including resistance to

Table 3
Genes predicted to confer disease resistance within the interval of the major QTL detected on Chr03: 25.59 to 29.10 Mbps ('Texas' genome v3.0-F1).

Description	Gene ID
2-methylene-furan-3-one reductase	TexasF1_G13611; TexasF1_G13632
Allene oxide cyclase	TexasF1_G13132
Altered xyloglucan 4-like	TexasF1_G13574
Cinnamoyl-CoA reductase-like SNL6	TexasF1_G13148; TexasF1_G13627
Early nodulin-like protein 20	TexasF1_G13485; TexasF1_G13495
GDSL esterase/lipase	TexasF1_G13212; TexasF1_G13616; TexasF1_G13617
Glycine-rich protein	TexasF1_G13473
HIPL1 protein	TexasF1_G13381
Monodehydroascorbate reductase 4	TexasF1_G13633
MYB domain protein 30	TexasF1_G13432
Pathogenesis-related thaumatin superfamily protein (thaumatin-like protein)	TexasF1_G13522
Pectin methylesterase 31	TexasF1_G13474
PR5-like receptor kinase (leaf rust 10 disease-resistance locus receptor-like protein kinase-like 2.5)	TexasF1_G13368; TexasF1_G13370; TexasF1_G13371
Proline dehydrogenase 2	TexasF1_G13172
Proteasome maturation factor UMP1	TexasF1_G13137
Receptor-like protein kinase	TexasF1_G13149; TexasF1_G13197; TexasF1_G13247; TexasF1_G13248; TexasF1_G13249; TexasF1_G13250; TexasF1_G13251; TexasF1_G13252; TexasF1_G13253; TexasF1_G13256; TexasF1_G13258; TexasF1_G13264; TexasF1_G13265; TexasF1_G13266; TexasF1_G13267; TexasF1_G13268; TexasF1_G13271; TexasF1_G13272; TexasF1_G13294; TexasF1_G13413; TexasF1_G13523; TexasF1_G13586; TexasF1_G13592
Serine carboxypeptidase-like 25	TexasF1_G13298
Small GTP-binding protein	TexasF1_G13408
Transducin/WD40 repeat-like superfamily protein (ribosome biogenesis protein WDR12)	TexasF1_G13302
WRKY DNA-binding protein 72	TexasF1_G13407

diseases, to develop new technologies that increase breeding efficiency. However, despite the impact of diseases on almond production, no genetic studies linked to disease tolerance in almond breeding programs have been reported to date (Goonetilleke & Fernández i Martí, 2023). To the best of our knowledge, this is the first time that an almond disease (RLB) has been studied through QTL mapping. RLB is considered one of the main diseases affecting almond crops in the Mediterranean and Middle East countries, making the development of more tolerant cultivars a key target in almond breeding programs (Batlle et al., 2017). However, despite extensive field documentation of different levels of cultivar susceptibility, little is known about the genetic control of RLB tolerance in almonds (Egea et al., 1984; Saad & Masannat, 1997; Heydarian & Moradi, 2005; Ollero-Lara et al., 2019; Miarnau et al., 2021). In this study, we investigated the genetic basis of RLB tolerance using the almond Axiom™ 60K SNP array (Duval et al., 2023) platform, an excellent source for genotyping and later performing QTL and genome-wide association studies in the species (Pérez de los Cobos et al., 2023). The number of mapped markers in both parentals and the T×V maps was within the range previously described for saturated maps constructed using this SNP array (Duval et al., 2023) and genotyping-by-sequencing technologies (Goonetilleke et al., 2018), and surpassed those maps constructed using SSR markers (Sánchez-Pérez et al., 2007; Font i Forcada et al., 2012; Fernández i Martí et al., 2013). This efficiency highlights this new array as a wonderful tool to conduct genetic analyses and develop molecular markers for assisted selection in almond breeding programs, given the elevated marker saturation.

The different levels of disease incidence and severity across almond germplasm suggest a polygenetic component regulating tolerance at the cultivar level. In this work, two cultivars were considered: 'Tarraco', which previously showed high susceptibility to RLB, and 'Vairo' which demonstrated a certain level of tolerance compared with other almond cultivars (Zúñiga et al., 2019; Miarnau et al., 2021). The behavior of these cultivars was confirmed in this study, where 'Tarraco' presented infection rates higher than 'Vairo'. Within the individuals of the F_1 population, a wide range of segregation in disease tolerance levels was observed, with individuals exhibiting both higher and lower susceptibility levels than parentals. However, only a few individuals presented incidence and severity indexes below those of 'Vairo' (the tolerant cultivar), with the individuals of the population showing clear segregation towards higher disease susceptibility. This suggests the presence of alleles associated with disease tolerance that likely exhibit a recessive effect.

Additionally, correlations between disease indicators (incidence and severity) across years were low. This finding is consistent with other studies that evaluated fungal infections in segregating populations (Pacheco et al., 2014). Considering that RLB infections rely on the presence of airborne ascospores, disease levels can be highly influenced by the meteorological conditions that determine inoculum development and outbreaks (Pons-Solé et al., 2023). For example, in 2020, the period from April to June experienced higher rainfall (215 mm) compared to other phenotyped years (134, 85, and 91 mm in 2018, 2019, and 2022, respectively) (Statistical Yearbook of Catalonia, 2024). In 2020, higher disease levels were observed which could be linked to a higher inoculum presence in the field. *Polystigma amygdalinum* has been reported to produce severe ascospore outbreaks under favorable conditions, such as mild temperatures and humidity, particularly following rain events (Banihashemi 1990; Zúñiga et al., 2020; Miarnau et al., 2021; Pons-Solé et al., 2023; Pons-Solé et al., 2024). This influential effect of environmental conditions could be also responsible for the differences in susceptibility observed at the cultivar level in some studies. Hence, Ollero-Lara et al. (2019) reported 'Tarraco' as tolerant when compared to 'Guara', while this work and previous research (Miarnau et al., 2021) found a high susceptibility to RLB for 'Tarraco'.

RLB disease development is highly influenced by environmental conditions affecting inoculum dynamics and disease progress. However, a moderate heritability was observed for RLB tolerance in the studied population ($H^2 = 0.55$ and 0.66 for incidence and severity, respectively), which highlights its inheritance control and the possibility of carrying out genetic analyses. Additionally, the different levels of susceptibility to RLB found across almond germplasm (Egea et al., 1984; Ollero-Lara et al., 2019; Miarnau et al., 2021), along with the distribution of disease indexes in the T×V population, may indicate the polygenic control of the disease. This hypothesis seemed supported by our current QTL analysis, which revealed the presence of several QTLs distributed among various genomic regions. Nevertheless, only one QTL (*qP-RLB3.1*^{m}) demonstrated stability across different years, parental cultivars, and disease incidences. This stable QTL, located on LG3, accounted for 18 to 31% of the phenotypic variation, with the QTL peak around 27 Mbp (Chr3). Notably, *qP-RLB3.1*^{m} was found in the same region where a previous QTL for resistance to sharka disease (plum pox virus; PPV) was reported in apricot (Lambert et al., 2007). Moreover, the detection of this main QTL in both parental cultivars, despite their different genetic backgrounds, suggests that this could be a potential region harboring key gene(s) controlling RLB tolerance in almond germplasm, which once validated, could be targeted in breeding programs.

Besides *qP-RLB3.1*^{m}, additional minor QTLs were identified in various genome regions, overlapping with regions containing QTLs associated with other plant diseases previously reported in other species. This is the case of *qP-RLB1.1*, located on LG1 (Chr01: 9.52-12.25 Mbps), that overlapped with PPV, *Monilinia* spp., and *Xanthomonas* spp. related QTLs previously detected in other *Prunus* species (Lambert et al., 2007; Yang et al., 2013; Martínez-García et al., 2013; Pacheco et al., 2014). Similarly, the QTLs identified on LGs 7 (*qP-RLB7.1*) and 8 (*qP-RLB8.1* and *qP-RLB8.2*) in this work have been previously documented in other

Prunus populations investigated for brown rot resistance (Pacheco et al., 2014). However, none of these QTLs exhibited stability over the years, indicating the impact of environmental conditions on their expression. These conditions are correlated with varying disease incidences, potentially linked to the activation of specific genes with minor effects on increasing tolerance levels.

The consistent co-localization of *qP-RLB3.1*^{m} across years, maps, and disease indexes highlights this region as crucial for identifying candidate genes linked to RLB resistance in almonds. Within this region, several gene families associated with pathogen resistance in plants have been identified. This is the case of receptor-like proteins (RLP), which have been identified as providing resistance to certain fungal pathogens such as *Fulvia fulvum* (Cooke) Cif., *Plasmopara viticola* (Berk. & M.A. Curtis) Berl. & De Toni, and *Pyricularia grisea* Cooke ex Sacc. (Krujit et al., 2005; Li et al., 2009; Lan et al., 2019). These genes play a pivotal role in sensing and interpreting external stimuli, subsequently activating relevant downstream signaling pathways, including defense mechanisms. Within *qP-RLB3.1*^{m}, 26 genes annotated as RLP have been observed. It is important to highlight TexasF1_G13368, TexasF1_G13370, and TexasF1_G13371, which were annotated as PR5-like receptor kinase (leaf rust 10 disease-resistance locus receptor-like kinase), and whose expression has been reported in various plant species during defense responses (Wang et al., 1996; Yao et al., 2020; Massodi et al., 2022). This suggests a role of this gene in the perception of microbial signals and makes it a good candidate associated with the phenotypic variation of the QTL. Other potentially important genes identified within this QTL interval include TexasF1_G13148 and TexasF1_G13627, both annotated as members of the cinnamoyl-CoA reductase-like family. These genes have been documented to confer immunity to *Xanthomonas oryzae* pv. *oryzae* in rice plants by modulating lignin content (Bart et al., 2010; Cui et al., 2022). This is particularly relevant in RLB management, as lignin biosynthesis has been identified as a crucial mechanism for inhibiting fungal growth in almond, with lignin deposition observed in fungal-colonized areas in highly tolerant cultivars such as 'Mardía' (Zúñiga et al., 2019).

Additional genes with predicted functions linked to disease resistance, such as 2-methylene-furan-3-one reductase, were identified within *qP-RLB3.1*^{m} (TexasF1_G13611; TexasF1_G13632). These genes are involved in the synthesis of volatile furaneol, an organic compound known to induce defense priming and enhance resistance against pathogens (Quintana-Rodriguez et al., 2014; Peinado-Guevara et al., 2017; Rego et al., 2022). This variation in disease susceptibility among individuals within the population and almond cultivars could potentially be associated with these genes. Similarly, other candidate resistance genes found within the QTL interval included the pathogenesis-related thaumatin-like protein (TexasF1_G13522) that has been reported to mediate against leaf rust fungus (Petre et al., 2011; Zhang et al., 2018), the allene oxide cyclase (TexasF1_G13132) that promotes the expression of genes associated with disease resistance in sugarcane (Sun et al., 2023), or GDSL-type esterase/lipase genes that promote defense against pathogens in several plant species (Hong et al., 2008; Gao et al., 2017; Ji et al., 2023).

In addition to identifying candidate genes within *qP-RLB3.1*^{m}, the discovery of alleles from this genomic region is valuable for selecting individuals with greater tolerance to RLB infection. In the T×V population, a promising breeding allele linked to reduced disease incidence (AA|AA for AX-586074286|AX-586076177 genotypes, respectively) was identified. Furthermore, this allele was validated in the germplasm, as 'Mardía', an almond cultivar known for its high tolerance to RLB (highly superior to any other almond cultivar) (Zúñiga et al., 2019; Miarnau et al., 2021), exhibited the same genotype as individuals in the population with the lowest infection rates. Therefore, despite variations in disease incidence due to environmental conditions, the SNPs used for haplotype construction in this study can effectively distinguish between different susceptibility levels in the almond germplasm. This suggests that marker development focusing on this allele may hold considerable promise for applications in almond breeding.

5. Conclusions

This study investigated the genetics of RLB in almonds through QTL analysis for the first time. The varying levels of disease tolerance observed in the individuals of the F_1 population ('Tarraco' × 'Vairo') suggested a genetic control of RLB. A stable QTL, *qP-RLB3.1*^{m}, was identified in the lower region of LG3 across all four phenotyped years, explaining up to 31% of the phenotypic variation. Haplotype analysis of this major QTL revealed that individuals with the lowest disease incidence shared a common haplotype. This haplotype, consisting of two SNP makers, was also found in 'Mardía', the almond cultivar with the highest disease tolerance, indicating a potential target for breeding. Moreover, 42 genes associated with pathogen resistance were identified as potential candidates for RLB tolerance within *qP-RLB3.1*^{m} region. Thus, this research serves as a foundation for advancing the breeding of almond cultivars with enhanced resistance to RLB.

Funding sources

This project was funded by the 'Agencia Estatal de Investigación' (AEI) (Ministry of Science, Innovation, and Universities; Government of Spain) through grants RTA2017-00084-00-00, PID2020-114648RR-C31 and PID2020-118612RR-I00. All authors except GPS, LT, and NR were partially supported by CERCA Program, Generalitat de Catalunya. GPS was supported by a predoctoral grant (PRE2018-085207) from AEI, Spain. NR was supported by INVESTIGO Program (100049ID3), Generalitat de Catalunya.

Data statement

All data is available in the tables and figures within the manuscript and supplementary material.

CRediT authorship contribution statement

Alejandro Calle: Writing – original draft, Software, Investigation, Formal analysis, Data curation. **Gemma Pons-Solé:** Writing – review & editing, Data curation. **Núria Real:** Writing – review & editing, Data curation. **Jordi Luque:** Writing – review & editing, Resources, Data curation, Investigation. **Iban Eduardo:** Writing – review & editing, Data curation. **Laura Torguet:** Writing – review & editing, Data curation, Investigation. **Ignasi Batlle:** Writing – review & editing, Data curation. **Xavier Miarnau:** Writing – review & editing, Resources, Data curation, Conceptualization, Investigation.

Declaration of competing interest

The authors declare that they have no conflict of interest.

Supplementary materials

Supplementary material associated with this article can be found, in the online version, at doi:10.1016/j.scienta.2024.113901.

Data availability

Data will be made available on request.

References

Aranzana, M.J., Decroocq, V., Dirlewanger, E., Eduardo, I., Gao, Z.S., Gasic, K., Iezzoni, A., Jung, S., Peace, C., Prieto, H., Tao, R., Verde, I., Abbott, A.G., Arús, P., 2019. *Prunus* genetics and applications after *de novo* genome sequencing: achievements and prospects. Hortic. Res. 6, 58. https://doi.org/10.1038/s41438-019-0140-8.

Banihashemi, Z., 1990. Biology and control of *Polystigma ochraceum*, the cause of almond red leaf blotch. Plant Pathol. 39, 309–315. https://doi.org/10.1111/j.1365-3059.1990.tb02508.x.

Bart, R.S., Chern, M., Vega-Sánchez, M.E., Canlas, P., Pc, R., 2010. Rice *Snl6*, a cinnamoyl-CoA reductase-like gene family member, is required for nh1-mediated immunity to Xanthomonas oryzae pv. oryzae. PLoS Genet. 6 (9), e1001123. https://doi.org/10.1371/journal.pgen.1001123.

Bates, D., Mächler, M., Bolker, B., Walker, S., 2015. Fitting linear mixed-effects models using lme4. J. Stat. Softw. 67 (1), 1–48. https://doi.org/10.18637/jss.v067.i01.

Batlle, I., Dicenta, F., Socias i Company, R., Gradziel, T.M., Wirthensohn, M., Duval, H., Vargas, F.J., 2017. Classical genetics and breeding. Socias i Company R, Gradziel TM Almonds: Botany, Production and Uses. CABI International. USA, pp. 111–148.

Cannon, P.E., 1996. Systematics and diversity of the Phyllachoroceae associated with Rosaceae, with a monograph of *Polystigma*. Mycol. Res. 100, 1409–1427. https://doi.org/10.1016/S0953-7562(96)80072-4.

Castanera, R., de Tomás, C., Ruggieri, V., Vicient, C., Eduardo, I., Aranzana, M.J., Arús, P., Casacuberta, J.M., 2024. A phased genome of the highly heterozygous 'Texas' almond uncovers patterns of allele-specific expression linked to heterozygous structural variants. Hortic. Res. 11 (6), uhae106. https://doi.org/10.1093/hr/uhae106.

Cui, W., Zhuang, Z., Jiang, P., Pan, J., Zhao, G., Xu, S., Shen, W., 2022. Characterization, expression profiling, and biochemical analyses of the cinnamoyl-CoA reductase gene family for lignin synthesis in alfalfa plants. Int. J. Mol. Sci. 23 (14), 7762. https://doi.org/10.3390/ijms23147762.

Doyle, J.J., Doyle, J.L., 1990. A rapid total DNA preparation procedure for fresh plant tissue. Focus 12, 13–15. https://doi.org/10.4236/ajps.2014.55072. . (Madison).

Duval, H., Coindre, E., Ramos-Onsins, S.E., Alexiou, K.G., Rubio-Cabetas, M.J., Martínez-García, P.J., Wirthensohn, M., Dhingra, A., Samarina, A., Arús, P., 2023. Development and evaluation of an axiomTM 60K SNP array for almond (*Prunus dulcis*). Plants 12 (2), 242. https://doi.org/10.3390/plants12020242.

Egea L., García J.E., Egea J., Berenguer T. (1984) Premières observations sur une collection de 81 variétés d'amandiers situé dans le sud-est espagnol. Options Méditerranéennes 84: 13-25.

European Commission (2019) The european green deal. 2024 Retrieved from https://ec.europa.eu/info/sites/info/files/european-green-deal-communication_en.pdf.

Fernández i Martí, A., Font i Forcada, C., Socias i Company, R., 2013. Genetic analysis for physical nut traits in almond. Tree Genet. Genomes 9 (2), 455–465.

Font i Forcada, C., Fernández i Martí, A., Socias i Company, R.S., 2012. Mapping quantitative trait loci for kernel composition in almond. BMC Genet. 13 (1), 1–9. https://doi.org/10.1186/1471-2156-13-47.

Gao, M., Yin, X., Yang, W., Lam, S.M., Tong, X., Liu, J., Wang, X., Li, Q., Shui, G., He, Z., 2017. GDLS lipases modulate immunity through lipid homeostasis in rice. PLoS Pathog. 13 (11), e1006724. https://doi.org/10.1371/journal.ppat.1006724.

Goonetilleke, S.N., Fernández i Martí, Á., 2023. Discovery of quantitative trait loci for nut and quality traits in almond. In: Sánchez-Pérez, R, Fernandez i Marti, A, Martinez-Gomez, P (Eds.), The Almond Tree Genome. Compendium of Plant Genomes. Springer, Cham.

Goonetilleke, S.N., March, T.J., Wirthensohn, M.G., Arús, P., Walker, A.R., Mather, D.E., 2018. Genotyping by sequencing in almond: SNP discovery, linkage mapping, and marker design. G3 Genes Genomes Genet. 8 (1), 161–172. https://doi.org/10.1534/g3.117.300376.

Grattapaglia, D., Sederoff, R., 1994. Genetic linkage maps of *Eucalyptus grandis* and *Eucalyptus urophylla* using a pseudo-testcross: mapping strategy and RAPD markers. Genetics 137 (4), 1121–1137. https://doi.org/10.1093/genetics/137.4.1121.

Habibi, A., Banihashemi, Z., 2016. Mating system and role of pycnidiospores in biology of *Polystigma amygdalinum*, the causal agent of almond red leaf blotch. Phytopathol. Mediterr. 55, 98–108.

Heydarian, A., Moradi, H., 2005. Relative resistance of selected almond cultivars to the causal agent of red leaf blotch disease in Chahar Mahal-V A-Bakhtiari Province. Iran. J. Plant Pathol. 41, 157–169.

Hong, J.K., Choi, H.W., Hwang, I.S., Kim, D.S., Kim, N.H., Choi, D.S., Kim, Y.J., Hwang, B.K., 2008. Function of a novel GDSL-type pepper lipase gene, CaGLIP1, in disease susceptibility and abiotic stress tolerance. Planta 227, 539–558. https://doi.org/10.1007/s00425-007-0637-5.

Jansen, R.C., 1994. Controlling the type I and type II errors in mapping quantitative trait loci. Genetics 138 (3), 871–881. https://doi.org/10.1093/genetics/138.3.871.

Ji, Z., Wang, M., Zhang, S., Du, Y., Cong, J., Yan, H., Guo, H., Xu, B., Zhou, Z., 2023. GDSL esterase/lipase GELP1 involved in the defense of apple leaves against *Colletotrichum gloeosporioides* infection. Int. J. Mol. Sci. 24 (12), 10343. https://doi.org/10.3390/ijms241210343.

Jung, S., Lee, T., Cheng, C.H., Buble, K., Zheng, P., Yu, J., Humann, J., Ficklin, S.P., Gasic, K., Scott, K., Frank, M., Ru, S., Hough, H., Evans, K., Peace, C., Olmstead, M., DeVetter, L.W., McFerson, J., Coe, M., Wegrzyn, J.L., Staton, M.E., Abbott, A.G., Main, D., 2019. 15 years of GDR: new data and functionality in the genome database for rosaceae. Nucleic Acids Res. 8 (47), 1137–1145. https://doi.org/10.1093/nar/gky1000.

Kosambi, D.D., 1944. The estimation of map distances from recombination values. Ann. Eugen. 12, 172–175. https://doi.org/10.1111/j.1469-1809.1943.tb02321.x.

Kruijt, M., De Kock, M., De Wit, P., 2005. Receptor-like proteins involved in plant disease resistance. Mol. Plant Pathol. 6, 85–97. https://doi.org/10.1016/j.pmpp.2023.102004.

Lan, X., Liu, Y., Song, S., Yin, L., Xiang, J., Qu, J., Lu, J., 2019. *Plasmopara viticola* effector PvRXLR131 suppresses plant immunity by targeting plant receptor-like kinase inhibitor BKI1. Mol. Plant Pathol. 20 (6), 765–783. https://doi.org/10.1111/mpp.12790.

Lander, E.S., Botstein, D., 1989. Mapping Mendelian factors underlying quantitative traits using RFLP linkage maps. Genetics 121, 185–199. https://doi.org/10.1093/genetics/121.1.185.

Lambert, P., Dicenta, F., Rubio, M., Audergon, J.M., 2007. QTL analysis of resistance to sharka disease in the apricot (*Prunus armeniaca* L.) 'Polonais' × 'Stark Early Orange' F1 progeny. Tree Genet. Genomes 3, 299–309. https://doi.org/10.1007/s11295-006-0069-6.

Li, H., Zhou, S.Y., Zhao, W.S., Su, S.C., Peng, Y.L., 2009. A novel wall-associated receptor-like protein kinase gene, *OsWAK1*, plays important roles in rice blast disease resistance. Plant Mol. Biol. 69, 337–346. https://doi.org/10.1007/s11103-008-9430-5.

López-López, M., Calderón, R., González-Dugo, V., Zarco-Tejada, P., Fereres, E., 2016. Early detection and quantification of almond red leaf blotch using high-resolution hyperspectral and thermal imagery. Remote Sens. 8, 276. https://doi.org/10.3390/rs8040276 (Basel).

López-Moral, A., Agustí-Brisach, C., Ruiz-Prados, M.D., Lovera, M., Luque, F., Arquero, O., Trapero, A., 2022. Biological and urea treatments reduce the primary inoculum of red leaf blotch of almond caused by *Polystigma amygdalinum*. Plant Dis. 107, 2088–2095. https://doi.org/10.1094/PDIS-04-22-0957-RE.

Martínez-García, P.J., Parfitt, D.E., Bostock, R.M., Fresnedo-Ramírez, J., Vazquez-Lobo, A., Ogundiwin, E.A., Gradziel, T., Crisosto, C., 2013. Application of genomic and quantitative genetic tools to identify candidate resistance genes for brown rot resistance in peach. PLoS One 8 (11), e78634. https://doi.org/10.1371/journal.pone.0078634.

Masoodi, K.Z., Ahmed, N., Mir, M.A., Bhat, B., Shafi, A., Mansoor, S., Rasool, R.S., Yaseen, M.Y., Dar, Z.A., Mir, J.I., Mudasir Andrabi, S., Ganai, N.A., 2022. Comparative transciptomics unravel new genes imparting scab resistance in apple (*Malus x domestica* Borkh. Funct. Integr. Genom. 22, 1315–1330. https://doi.org/10.1007/s10142-022-00889-x.

Miarnau, X., Zazurca, L., Torguet, L., Zúñiga, E., Batlle, I., Alegre, S., Luque, J., 2021. Cultivar susceptibility and environmental parameters affecting symptom expression of red leaf blotch of almond in Spain. Plant Dis. 105, 940–947. https://doi.org/10.1094/PDIS-04-20-0869-RE.

Ollero-Lara, A., Agustí-Brisach, C., Lovera, M., Roca, L.F., Arquero, O., Trapero, A., 2019. Field susceptibility of almond cultivars to the four most common aerial fungal diseases in southern Spain. Crop Prot. 121, 18–27. https://doi.org/10.1016/j.cropro.2019.03.005.

Pacheco, I., Bassi, D., Eduardo, I., Ciacciulli, A., Pirona, R., Rossini, L., Vecchietti, A., 2014. QTL mapping for brown rot (*Monilinia fructigena*) resistance in an intraspecific peach (*Prunus persica* L. batsch) F1 progeny. Tree Genet. Genomes 10, 1223–1242. https://doi.org/10.1007/s11295-014-0756-7.

Peinado-Guevara, L.I., López-Meyer, M., López-Valenzuela, J.A., Maldonado-Mendoza, I. E., Galindo-Flores, H., Campista-León, S., Medina-Godoy, S., 2017. Comparative proteomic analysis of leaf tissue from tomato plants colonized with *Rhizophagus irregularis*. Symbiosis 73, 93–107. https://doi.org/10.1007/s13199-016-0470-3.

Pérez de los Cobos, F., Coindre, E., Dlalah, N., Quilot-Turion, B., Batlle, I., Arús, P., Eduardo, I., Duval, H., 2023. Almond population genomics and non-additive GWAS reveal new insights into almond dissemination history and candidate genes for nut traits and blooming time. Hortic. Res. 10, uhad193. https://doi.org/10.1093/hr/uhad193.

Petre, B., Major, I., Rouhier, N., Duplessis, S., 2011. Genome-wide analysis of eukaryote thaumatin-like proteins (TLPs) with an emphasis on poplar. BMC Plant Biol. 11, 33. https://doi.org/10.1186/1471-2229-11-33.

Pons-Solé, G., Miarnau, X., Torguet, L., Lázaro, E., Vicent, A., Luque, J., 2023. Airborne inoculum dynamics of *Polystigma amygdalinum* and progression of almond red leaf blotch disease in Catalonia, NE Spain. Ann. Appl. Biol. 183, 33–42. https://doi.org/10.1111/aab.12831.

Pons-Solé, G., Miarnau, X., Torguet, L., Lázaro, E., Vicent, A., Luque, J., 2024. Modeling the airborne inoculum of *Polystigma amygdalinum* to optimize fungicide programs against almond red leaf blotch. Plant Dis. 108, 737–745. https://doi.org/10.1094/PDIS-08-23-1540-RE.

Quintana-Rodriguez, E., Morales-Vargas, A.T., Molina-Torres, J., Ádame-Álvarez, R.M., Acosta-Gallegos, J.A., Heil, M., 2014. Plant volatiles cause direct, induced and associational resistance in common bean to the fungal pathogen *Colletotrichum lindemuthianum*. J. Ecol. 103, 250–260. https://doi.org/10.1111/1365-2745.12340.

R Core Team (2021) R: A language and environment for statistical computing. R Foundation for Statistical Computing, Vienna, Austria. https://www.R-project.org/.

Rego, A.P.B., Mora-Ocampo, I.Y., Pirovani, C.P., Luz, E., Corrêa, R.X., 2022. Protein level defense responses of *Theobroma cacao* interaction with *Phytophthora palmivora*. Front. Agronomy 4, 836360. https://doi.org/10.3389/fagro.2022.836360.

Revelle, W., 2024. psych: Procedures for Psychological, Psychometric, and Personality Research. Northwestern University, Evanston, Illinois. R package version 2.4.6. https://CRAN.R-project.org/package=psych.

Saad A.T., Masannat K. (1997) Economic importance and cycle of *Polystigma ochraceum*, causing red leaf blotch disease of almond, in Lebanon. Bulletin OEPP/EPPO 27: 481-485.

Sánchez-Pérez, R., Howad, W., Dicenta, F., Arús, P., Martínez-Gómez, P., 2007. Mapping major genes and quantitative trait loci controlling agronomic traits in almond. Plant Breed. 126 (3), 310–318. https://doi.org/10.1111/j.1439-0523.2007.01329.x.

S.Y. Catalonia (2024). Precipitation. Monthly and annual precipitations. Counties. Generalitat of Catalonia. https://www.idescat.cat/indicadors/?id=aec&n=15195&lang=en&t=202200.

Sun, T., Chen, Y., Feng, A., Zou, W., Wamg, D., Lin, P., Chen, Y., You, C., Que, Y., Su, Y., 2023. The allene oxide synthase gene family in sugarcane and its involvement in disease resistance. Ind. Crops Prod. 192, 116136. https://doi.org/10.1016/j.indcrop.2022.116136.

ThermoFisher. (2017). Axiom Analysis Suite 3.1—User Manual. Carlsbad, CA (USA).
Torguet, L., Zazurca, L., Martínez, G., Pons-Solé, G., Luque, J., Miarnau, X., 2022. Evaluation of fungicides and application strategies for the management of the red leaf blotch disease of almond. Horticulturae 8 (6), 501. https://doi.org/10.3390/horticulturae8060501.
van Ooijen, J.W., 1992. Accuracy of mapping quantitative trait loci in autogamous species. Theor. Appl. Genet. 84, 803–811. https://doi.org/10.1007/BF00227388.
van Ooijen, J.W., 2009. MapQTL® 6, Software for the Mapping of Quantitative Trait Loci in Experimental Populations of Diploid Species. Kyazma B.V., Wageningen, Netherlands.
van Ooijen J.W. (2018) JoinMap® 5, Software for the calculation of the genetic linkage maps in experimental populations of diploid species. Kyazma B.V., Wageningen, Netherlands.
Vargas, F., Romero, M., Clavé, J., Vergés, J., Santos, J., Batlle, I., 2008. 'Vayro', 'Marinada', 'Constantí', and 'Tarraco' almonds. HortSciences 43 (2), 535–537. https://doi.org/10.21273/HORTSCI.43.2.535.
Voorrips, R.E., 2002. MapChart: software for the graphical presentation of linkage maps and QTLs. J. Hered. 93 (1), 77–78. https://doi.org/10.1093/jhered/93.1.77.
Wang, X., Zafian, P., Choudhary, M., Lawton, M., 1996. The PR5K receptor protein kinase from *Arabidopsis thaliana* is structurally related to a family of plant defense proteins. PNAS 93 (6), 2598–2602. https://doi.org/10.1073/pnas.93.6.2598.
Yang, N., Reighard, G., Ritchie, D., Okie, W., Gasic, K., 2013. Mapping quantitative trait loci associated with resistance to bacterial spot (*Xanthomonas arboricole* pv. *pruni*) in peach. Tree Genet. Genomes 9, 573–586. https://doi.org/10.1007/s11295-012-0580-x.
Yao, L., Li, Y., Ma, C., Tong, L., Du, F., Xu, M., 2020. Combined genome-wide association study and transcriptome analysis reveal candidate genes for resistance to *Fusarium* ear rot in maize. J. Integr. Plant Biol. 62 (10), 1535–1551. https://doi.org/10.1111/jipb.12911.
Zhang, J., Wang, F., Liang, F., Zhang, Y., Ma, L., Wang, H., Liu, D., 2018. Functional analysis of a pathogenesis-related thaumatin-like protein gene *TaLr35PR5* from wheat induced by leaf rust fungus. BMC Plant Biol. 18, 76. https://doi.org/10.1186/s12870-018-1297-2.
Zúñiga, E., Luque, J., Martos, S., 2019. Lignin biosynthesis as a key mechanism to repress *Polystigma amygdalinum*, the causal agent of the red leaf blotch disease in almond. J. Plant Physiol. 236, 96–104. https://doi.org/10.1016/j.jplph.2019.03.004.
Zúñiga, E., Romero, J., Ollero-Lara, A., Lovera, M., Arquero, O., Miarnau, X., Torguet, L., Trapero, A., Luque, J., 2020. Inoculum and infection dynamics of *Polystigma amygdalinum* in almond orchards in Spain. Plant Dis. 104, 1239–1246. https://doi.org/10.1094/PDIS-07-19-1406-RE.